Sequestering and metamorphosis of molecular nitrogen at ambient conditions: role of bonding and back-bonding

Ratan Logdi ,[†] Arijit Bag,[*,‡] and Ashwani K. Tiwari[*,†]

†*Department of Chemical Sciences, Indian Institute of Science Education and Research Kolkata, 741246,West-Bengal, India.*

‡*Department of Applied Chemistry, Maulana Abul Kalam Azad University of Technology West Bengal, 741249, West Bengal, India.*

E-mail: arijit.bag@makautwb.ac.in; ashwani@iiserkol.ac.in

Abstract

The optical absorbance behavior of a molecule during the reaction is yet to be explored due to the deficiency in the development of appropriate theoretical and experimental tools. In the present study, the Intrinsic Reaction Coordinate (IRC) trapping methodology is implemented in a new approach to capture the electronic motion during the nitrogen activation reaction by heterocyclic carbenes. This technique acts as a Handycam (*Molecular Handycam*) to shoot photographs of electrons in the event of a chemical reaction beyond Born-Oppenheimer approximation. The use of the newly designed molecular Handycam to analyse electron flow at the frontier molecular orbitals during the adduct formation reaction of molecular nitrogen with heterocyclic carbene corroborated that in the carbene $-N_2$ reaction, carbene operates as a σ $-$acceptor and π $-$donor where the bonding and the back bonding processes occur before and after the transition state of the reaction. There is a significant time delay between the

bonding and the back bonding process which implies that the bonding−back-bonding is not simultaneous events for this reaction. These findings ameliorate the DFT-based designing of heterocyclic carbenes to model a congenial catalyst for the sequestering of atmospheric nitrogen and its metamorphosis to ammonia at an ambient and metal-free condition. It is also brought to light that the optical absorption behavior of a molecule may change along the reaction path. Though molecular nitrogen, model carbene and the carbene−N_2 adduct are non-responsive to visible light, an evanescent optical absorbance in the visible region is observed during the chemical reaction.

1 Introduction

Understanding chemical reactions at the electronic level are the most desirable dream of a chemist. Electronic structure theories[1–4] and Quantum dynamics[5,6] are frequently employed to fulfill these requirements. However, the exact interpretation of a chemical reaction in terms of its electron flow during the bond breaking or bond making of a chemical reaction is a formidable task, particularly, where the Born−Oppenheimer approximation is not applicable and non-adiabatic quantum effects become predominant. To go beyond these issues, a combined electron and nuclear dynamics may be implemented as described by the time−dependent Schrödinger equation (TDSE) which corresponds to multicomponent equations of motion for the molecular wave-function. Unfortunately, an exact solution to these equations is only possible for a model system or a system of few electrons and nuclei in very low dimensions. To bring these limitations under control, an adept attempt has been contemplated within the applicable theoretical arena and technical territory without forcing further computational complexities. This methodology involves electronic structure analysis at variable geometry along the reaction path and is termed Intrinsic Reaction Coordinate trapping.[7]

Intrinsic Reaction Coordinate (IRC) is acquainted as the lowest energy path on the potential energy surface (PES) that connects the reactants to the product(s) through a

transition state. It is trivial to construct the intermediate geometries along the reaction path using available computational chemistry programs. By capturing and analyzing the electron density distribution of frontier molecular orbitals at different geometries along the reaction path, the exact electron flow of the reaction could be affirmed. A computation of time-dependent density distribution at these geometries will give the behavioural change in optical absorbance of the molecules along the reaction path. Since orbital pictures are taken at different geometries, the electron flow observed in this study will differ from electron dynamic calculations which operate within BO approximation. These new approaches to analyzing a chemical reaction are employed for the sequestering of atmospheric nitrogen employing DFT-based designed heterocyclic carbenes.

Fixation of atmospheric nitrogen in the form of ammonia at an ambient condition in a green chemical pathway is one of the biggest challenges for chemical researchers. This is extremely important for the advancement of fertilizer industries and chemical technology.[8] In nature, nitrogen fixation occurs primarily as ammonia by symbiotic and non-symbiotic microorganisms. Plants use this source of nitrogen for their growth. Thus, ammonia (NH_3) is a requisite chemical for fertilizer industries. It is also essential for dyes industries, explosive and resin production.[8] For ammonia synthesis, industries still depend on the celebrated Haber-Bosch process which requires high temperature and pressure.[8–10] Thus, modification of reaction conditions towards the ambient temperature and pressure will lead to a hugely energetic and economic profit for the respective industries and the society. In this respect, artificial nitrogen fixation is extremely important and considered a grand scientific problem as it will ease the ammonia synthesis from nitrogen and hydrogen.

Sequestering of atmospheric nitrogen by organometallic compounds[11–20] was studied widely. Organometallic compounds are also useful to seize N_2 and to convert it to ammonia at an ambient condition to find out alternative chemical pathways.[21] The N_2 fixation by the non-metallic process has also attracted attention very recently.[22–27] In this new research avenue with the rapid development of carbene chemistry and its applications,[7,28–38]

carbenes are the front runners for the candidature of the N_2 sequestering agent.[23]

The possibility of nitrogen fixation by carbene was first reported in 1964 by Moore *et al.*[39] It is exhibited that methylene reacts with N_2 in matrix solution to form diazomethane. In an isotope labeling experiment of the photolysis reaction, it is observed that methylene is produced from the diazirine or diazomethane which again reproduces diazomethane by the reaction of newly generated methylene with the neighboring nitrogen. This outcome asserted that the sequestering of nitrogen using carbene is feasible which was further strengthened by Shilov *et al.*[40] A similar kind of phenomenon was observed in the solution phase too.[41]

The reaction between carbene and N_2 is well investigated with the help of quantum chemical tools.[22,24,25] Liu *et al.* concluded from the experiments and theoretical studies that the thermal decomposition of diazirine compounds produces carbene and diazo compounds.[42] The formations of the diazo derivatives and carbene compounds are controlled by the effect of the substituents of the diazirines. The C_{60} probe was employed to confirm that carbene is produced in this reaction. It is affirmed that the rebound reaction of N_2 with carbene forms the diazo compounds.

Park *et al.*[25] sketched a pathway to use carbene as a catalyst for N_2 activation by employing DFT and *ab initio* calculations. In this study, the binding aptitude of N_2 with different carbenes was tested. Computed results showed that the electron-donating tendency of the central carbene carbon governs the sequestering of N_2. The stability of the carbene $-$ N_2 adduct is governed by the HOMO-LUMO energy gap of the carbene. Calculated results suggested that the cyclic diphospinocarbenes(PHC) is an affluent candidate for the fixation of N_2 and conversion of N_2 to NH_3. Another method is described by the same group where a carbene-based catalyst, bis-formyl-(PHC1) pyridine, is designed in such a fashion that two carbene moieties of this molecule are situated face to face and capable to bind N_2 from two opposite sides. This activated nitrogen is then converted to NH_3 by Cp_2^*Cr as a reducing agent and $LutH^+$ as proton sources. The mechanistic details of this process were demonstrated and revealed that the highest activation energy barrier is 28.5 kcal/mol.

The recent development of the frustrated Lewis pair (FLP) chemistry for small molecule activation has also attracted several research groups to employ FLP to activate N_2.[24,43–45] Carbene-boron is one such FLP that has been recognized as a significant candidate for sequestering of N_2.[43–45] In 2019, Zhu *et al.*[43] demonstrated an alternative N_2 fixation process by a newly designed carbene-boron FLP. In the case of N_2 fixation by carbene-boron FLP, one of the lone pairs of the N_2 is donated to the vacant p orbital of the boron atom of the carbene-boron compound and another lone pair of the N_2 simultaneously attacks the electron-deficient carbene carbon of the carbene-boron compound. This reaction is thermodynamically and kinetically favorable. The same group has also developed another type of carbene-boron FLP which is more efficient than the previous one to activate N_2.[44] This work is further extended by the same group[45] which showed that for N_2 fixation by carbene-boron FLP, the substituents on the boron atom plays a major role.

Shahriar *et al.* proposed N_2 activation by employing persistent carbene pair.[22] A similar kind of work on SO_2 fixation is reported recently by Logdi *et al.*[7] In this method, a pair of the same carbenes, as well as different carbenes, are equally effective for sequestering and complete conversion of SO_2. From these two studies,[7,22] it could be concluded that the use of persistent carbene pair may be more effective for small molecule activation and conversion. The mechanistic investigation of Shahriar *et al.* revealed that the reaction occurs through a diazoalkane intermediate.

In spite of considerable use of carbenes for CO_2 sequestering and conversion,[46–49] they were unable to attract significant importance for the SO_2 fixation process due to the instability of carbene $-$ SO_2 adduct.[37] Very recently we reported that the modeling of proper carbenes, particularly, N-heterocyclic carbenes, is effective for the sequestering and conversion of SO_2 to valuable chemicals.[7,37,38] These carbenes are also highly reactive to NO_2.[38] The success of these studies motivates us to extend our studies with these carbenes for N_2 activation. Since carbene $-$ SO_2 and carbene $-$ NO_2 reactions are barrierless processes and occur at room temperature, carbene $-$ N_2 reactions may occur at an ambient condition. We

further extended our quest to convert the captured N_2 to ammonia.

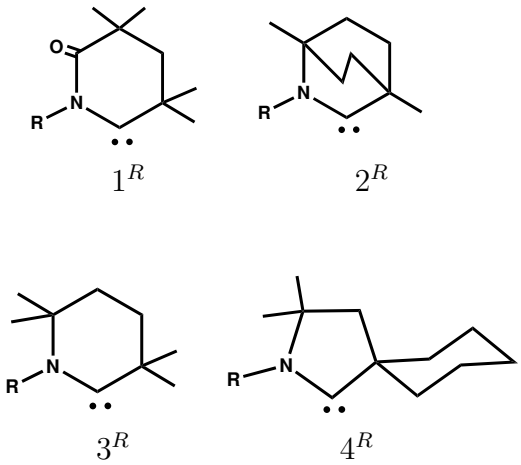

Figure 1: Selected N-heterocyclic carbenes for this study. ($R = CF_3$, CN, H, Me, OMe, Ph, tBu)

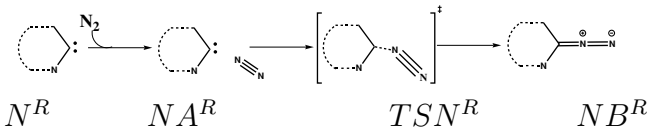

Figure 2: Schematic representation of N-heterocyclic carbene-N_2 reaction. ($N = 1, 2, 3, 4, 5$; $R = CF_3$, CN, H, Me, OMe, Ph, tBu)

To execute N_2 activation by carbene, initially four carbenes with seven substituents which are depicted in Figure 1, are tested. Carbene $-$ N_2 reaction is exhibited in Figure 2. The energy profile diagrams of the nitrogen activation process for different carbenes are constructed. Gibb's free energy values are used for this purpose. By the analysis of computed results, a model carbene is proposed which is used for further studies. The electronic mechanism of the nitrogen activation process by carbene is investigated using the IRC trapping method explained in our previous work.[7]

2 Methodology

The geometry optimization of all the compounds is carried out by employing M06-2X[37,38,50] functional adapting with 6-311++G** basis set for all of the atoms in Gaussian 09 pack-

age.[51] Frequency calculations are carried out with the same level of theory to ensure that reactants, products and intermediates do not have any imaginary frequency and transition state has only one mode of imaginary frequency. The IRC calculations are executed to assure the truthfulness of the transition states reported here. The changed geometries along the reaction path during the carbene$-N_2$ reaction are obtained from the IRC computation in both directions from the respective transition state. Time-dependent density functional theory (TD-DFT)[52] studies are also performed for all selected geometries along the reaction path. The thermodynamic properties are calculated with the assistance of frequency calculations. All the calculations are furnished at 298 K temperature.

3 Results and Discussion

Four different types of carbenes (1^R, 2^R, 3^R and 4^R) are chosen for the present study which are presented in Figure 1. For all types of carbenes, seven substituents ($R = CF_3$, CN, H, Me, OMe, Ph, tBu) are considered. The reaction of N_2 with these 28 carbenes is studied. The activation energies for these reactions are compared to find out the best carbene for N_2 activation. The orbital energies of carbenes and N_2 are analyzed to track down the electronic mechanism of nitrogen activation by carbene. How the substitutions at the nitrogen atom of the carbene frame affect the activation of the reaction is analyzed. On this basis carbene 5^R is modeled and continued for further investigation. The N_2 activation by carbene 5^R is found very good and better than all other carbenes considered earlier. Unfortunately, the Gibbs' free energy change for carbene $5^R - N_2$ reaction is positive. Therefore, we extended our studies in two different avenues. First, we follow the use of persistent carbene[7,22] to obtain a stable and thermodynamically favorable azo derivative. This technique is pursued due to the fact that the use of two carbenes for sequestering and conversation of SO_2 to valuable chemicals was proved effective.[7] In the inquisition of efficient carbenes for N_2 activation, we also followed the substitution of the heteroatom of the carbene backbone. This methodology

is accomplished owing to verifying the effect of substitution of the heteroatom nitrogen by phosphorus.

Both the aforementioned methods were found successful to obtain the activated nitrogen as a stable product. However, the substitution of hetero-nitrogen by phosphorus is more prolific to yield stable derivatives with lower activation energy. Thus, we continued our quest to convert activated nitrogen to ammonia with phosphorus substituted carbene. Electronic level investigations are carried out to explore the electron transfer mechanism of different reactions involved in the nitrogen activation process and the understanding of the role of the hetero atom and the substitution at the heteroatom.

3.1 Comparison of nitrogen activation efficacy of selected carbenes

First, the reactions of selected carbenes with nitrogen are performed and analyzed. To explore the substitution effect, the energy profile diagrams of different substitutions of the same carbene backbone are plotted together.

3.1.1 carbene 1^R

Carbene 1^R (Figure 3, $R = CF_3$, CN, H, Me, OMe, Ph, tBu) reacts with N_2 to form $1A^R$ which is in fact, a pre-complex formed due to the formation of weak hydrogen bonding between a nitrogen atom of N_2 molecule and the nearest hydrogen atom of the carbene molecule. The hydrogen bonding distances of different pre-complexes are within 2.7 Å to 2.9 Å. This step is endergonic for all carbenes. In the very next step, $1A^R$ converts to $1B^R$ through a transition state $TS1^R$. $1B^R$ is the activated complex that we are looking for. The energy required for the formation of $TS1^R$ from $1A^R$ is the activation energy for this step. In Figure 3, it is observed that the lowest activation energy is 22.7 kcal/mol which is for the CN substitution and the highest activation energy is 30.1 kcal/mol which is for the OMe substitution. The change in the activation energy of the reaction follows the

trend $CN < CF_3 < Ph < Me < H < tBu < OMe$. However, for all carbenes, the free energy change for the formation of $1B^R$ from the starting materials is positive. The order of stability of $1B^R$ follows the trend $CN > CF_3 > Ph > Me > tBu > H > OMe$ that is likely correlated to corresponding activation energies.

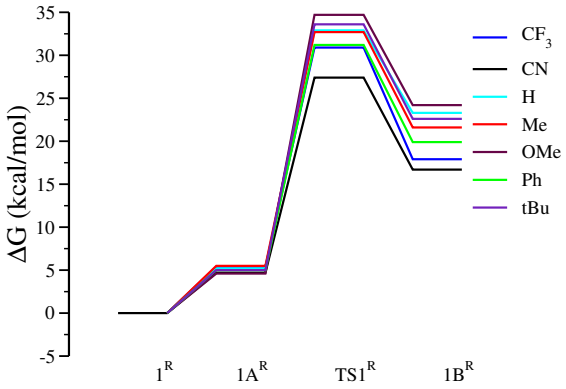

Figure 3: Energy profile diagram for the reaction of carbene 1^R ($R = CF_3$, CN, H, Me, OMe, Ph, tBu) with N_2.

3.1.2 carbene 2^R

The reaction between carbene 2^R ($R = CF_3$, CN, H, Me, OMe, Ph, tBu) and N_2 is presented in Figure 4. Here, $2A^R$ is the pre-complex. The activation energies for the formation of $2B^R$ from $2A^R$ follow the trend $CN < CF_3 < Ph < tBu < H < Me < OMe$ which is very similar to the trend observed for carbene 1^R except for Me, tBu and H. The order of the stabilities of activated complexes shows a different trend; $CN > CF_3 > Ph > OMe > H > Me > tBu$. The change in the order of stability may be due to the presence of the bridge at the carbene backbone. Here the steric factor of tBu reduces its stability. Additionally, due to the steric hindrance, the observed activation energies are higher for all substitutions corresponding to their 1^R analogue. The highest and the lowest activation energies for these carbenes are 41.0 kcal/mol and 30.1 kcal/mol. The highest activation energy is for the OMe substituents and the lowest activation energy is for the CN substituents. Interestingly, for the 1^R carbene, these two substituents show the highest and the lowest activation energy respectively.

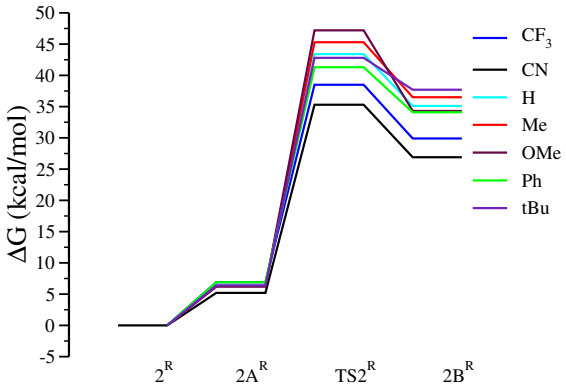

Figure 4: Energy profile diagram for the reaction of carbene 2^R ($R = CF_3$, CN, H, Me, OMe, Ph, tBu) with N_2.

3.1.3 carbene 3^R

The effect of substitutions ($R = CF_3$, CN, H, Me, OMe, Ph, tBu) to carbene 3^R is very similar to the other two carbenes discussed so far. The energy profile diagrams of carbene $3^R - N_2$ reactions are presented in Figure 5. The nature of pre-complexes formed for different substitutions ($3A^R$) are resembling previous carbenes. There is no significant change in the qualitative nature of the energy profile diagram. The free energy change for the formation of diazo derivative (carbene $- N_2$ adduct which is $3B^R$ in Figure 5) is positive for all substituents as observed for the earlier two carbenes . There are few changes in the order of activation energies and stabilities of diazo derivatives of different substituents. It is observed that for this carbene, the activation energy for the CF_3 substituent is less than the CN substituent by 0.6 kcal/mol. However, the CN substituted diazo derivative is more stable than that of the CF_3 substituted diazo derivative by 2.5 kcal/mol. The lowest and highest activation energies for 3^R carbene are 29.1 kcal/mol and 39.5 kcal/mol respectively corresponds to CF_3 and OMe substituents. The most stable diazo derivative is obtained for the CN substituent and the order of stability is $CN > CF_3 > tBu > Ph > Me > H > OMe$.

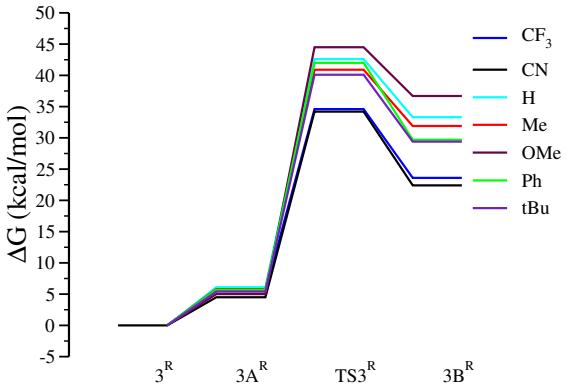

Figure 5: Energy profile diagram for the reaction of carbene 3^R ($R = CF_3$, CN, H, Me, OMe, Ph, tBu) with N_2.

3.1.4 carbene 4^R

The reaction of N_2 with 4^R carbene is presented in Figure 6. The formation of diazo derivative follows the same reaction path that is the formation of pre-complex ($4A^R$), transition state ($TS4^R$) and diazo derivative. These steps are endergonic for all substituents of this carbene. There is no significant change in the order of the activation energy barrier ($CN < CF_3 < Ph < Me < H < tBu < OMe$) and the order of stability ($CN > CF_3 > Ph > OMe > H > Me > tBu$). The lowest activation energy barrier is 30.5 Kcal/mol that is for 4^{CN} and the highest activation energy barrier is 45.8 Kcal/mol (for 4^{OMe}). For this carbene, CN substituent produces the most stable diazo derivative that is common for the other three carbenes too.

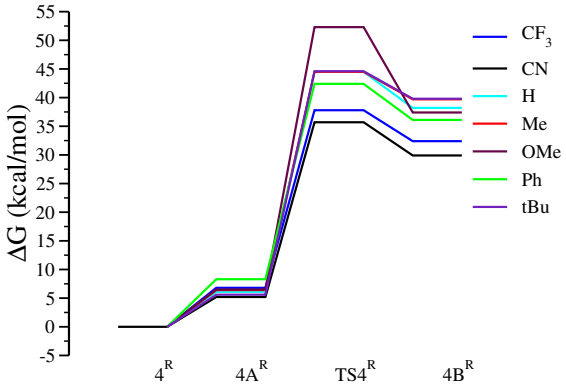

Figure 6: Energy profile diagram for the reaction of carbene 4^R ($R = CF_3$, CN, H, Me, OMe, Ph, tBu) with N_2.

3.2 Analysis of carbene $-$ N_2 reactions

The carbene -N_2 reactions were studied for 28 selected carbenes taking four different carbene backbones (1^R, 2^R, 3^R and 4^R) and seven different substituents (CF_3, CN, H, Me, OMe, Ph, tBu) are discussed in detail in the previous subsection. The observations are following

- All diazo derivatives are thermodynamically unstable ($\Delta G > 0$).
- The lowest activation energy is observed for 1^{CN} carbene.
- The activation energy and the thermodynamic stability of the diazo derivative depend on the chemical nature of the substitution at the hetero-atom.
- In most cases, the activation energy is the least and the stability of the diazo derivative is the highest for carbene 1^R of a particular substituent. This is true for almost all substituents.

Since the carbenes that are studied so far are associated with positive free energy change, these reactions are thermodynamically restricted. These reactions are only helpful to activate the N_2 molecule. Henceforth, these reactions should be coupled with other reactions to make a complete process thermodynamically feasible. In various ways, this could be achieved. The activated nitrogen may be converted to ammonia or other useable compounds that are associated with considerable negative free energy change. There is another way to stabilize the unstable diazo derivative. Selected chemicals may be employed that will play down the free energy of the reaction. The modeling of carbene may also lead to the thermodynamically acceptable production of diazo derivatives. These three approaches are followed in the present study.

To select an appropriate chemical to abate the reaction-free energy, the binding nature of the diazo derivative should be investigated. The effect of substitution to the carbene moiety is also analyzed to model carbenes that would be competent to produce diazo derivatives are associated with a negative free energy change.

3.2.1 Effect of substitution

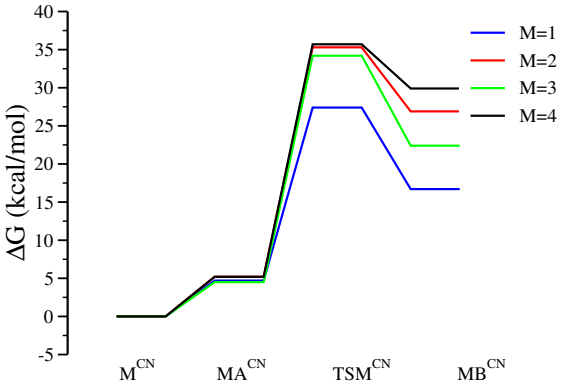

Figure 7: Energy profile diagram for the reaction of N_2 with four different carbenes (1^{CN}, 2^{CN}, 3^{CN} and 4^{CN}).

It is observed that the most stable diazo derivatives are produced for CN substituent of all four carbenes under study. The same is true for the activation energy of this process too, except for carbene 3^R where the activation energy of the CF_3 substituent is lower by only 0.6 kcal/mol than the CN substituent. Thus, the energy profile diagram for the CN substituents of four different carbenes are compared and presented in Figure 7. It is accomplished from figure 7 that the 1^{CN} carbene is the most fruitful considering both the factors (the activation energy and the stability of the diazo compound).

Therefore we investigate why 1^{CN} carbene is the affluent candidate for N_2 activation among all carbenes studied so far. From the structure of carbene 1^R presented in Figure 1, it is perceived that the carbene 1^R contains one $C = O$ group which is absent from the structure of the rest of the carbenes. The impact of the $C = O$ group on this process is yet to be brought to light. To cast more light on this matter, the molecular and electronic level inquisition is explored. The binding nature of carbene and N_2 is examined and the flow of electrons during this reaction is captured. The dominance of different substituents on the reactivity of carbene with nitrogen is also reviewed.

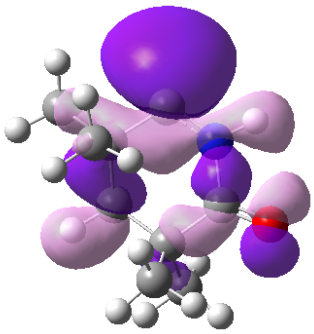

(a) 1^H HOMO (σ type)

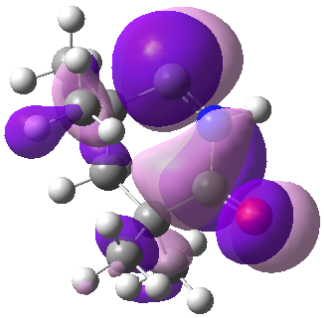

(b) 1^H LUMO (π type)

Figure 8: Frontier molecular Orbitals of 1^H carbene

3.2.2 Binding nature

It is well known that carbene may act as a σ-donor and π-acceptor. It may also act as a π-acceptor only. The exact role of the carbene depends on the nature of its counter reactant. It also depends on the structure of the carbene too. It is because the ground state of the small carbene is a triplet in nature whereas N-heterocyclic carbenes have a singlet ground state. There are two different possibilities of ground-state electronic distribution of singlet carbenes – the electron pair may occupy the σ orbital or the π orbital. The carbenes considered for this study, have the σ ground state. The frontier molecular orbitals of the ground state of 1^H carbene are presented in Figure 8. Depending upon the availability of the electron pair of the carbene and the electrophilicity difference between carbene and other reacting molecules, bonding and back bonding takes place. It is reported that the reaction of SO_2 with NHC occurs through the σ electron (σ^2) donation of NHC to the $\pi^{*(0)}$ of SO_2.[7] The reaction of NHC with NO_2 also occurs through σ electron (σ^2) donation of NHC. However, for this reaction, the NO_2 molecule is electronically excited to create a vacant σ orbital ($\sigma^1\sigma^{*0} \rightarrow \sigma^0\sigma^{*1}$).

The electronic configuration of the frontier molecular orbital of N_2 is $1\pi_u^4 3\sigma_g^2 1\pi_g^{*0} 3\sigma_u^{*0}$. The electronic probability distributions of these orbitals are presented in Figure 9 Thus, it is expected that the interaction between NHC and N_2 would be the same as it is observed for carbene – SO_2 reaction. Park *et al.*[25] come to a similar conclusion through a DFT

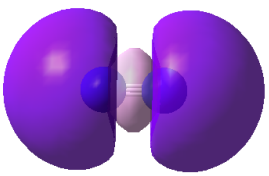

(a) N_2 HOMO

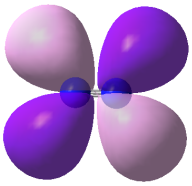

(b) N_2 LUMO (1)

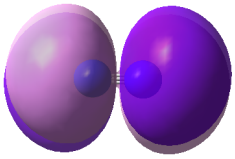

(c) N_2 LUMO (2)

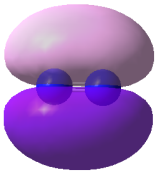

(d) N_2 HOMO-1 (1)

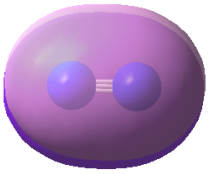

(e) N_2 HOMO -1 (2)

Figure 9: Frontier molecular Orbitals of N_2

study, while Grieve *et al.*[41] experienced a different conclusion. They observed that carbenes containing vacant σ orbital and filled π orbital ($\sigma^0\pi^2$ configuration) have better appetite towards N_2 and the electrophilicity of the carbenes governs the reaction. Since the singlet state of the carbenes are preferable for the reaction and $\sigma^0\pi^2$ configuration has better activity, it could be concluded that $3\sigma_g^2$ electron of N_2 is donated to the carbene first. It is exactly the reverse of the conclusion drawn by Park *et al.*[25] However, this is explainable. Though the nitrogen atom is highly electronegative, accepting an electron pair from carbene at a π^* orbital of a small molecule like N_2 with a triple bond, is improbable. Henceforth, the electronic mechanism of the carbene $-$ N_2 reaction is investigated.

3.2.3 Proposed electronic mechanism of carbene$-N_2$ reaction

To explicit the carbene $-$ N_2 reaction, the orbital energies of the frontier molecular orbitals of carbene (1^H) and N_2 molecule are compared and presented in Figure 10. In Figure 10, it is observed that the lowest energy vacant π^* orbital of N_2 has positive orbital energy.

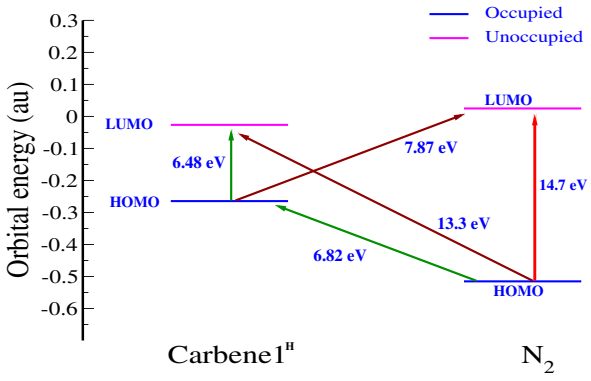

Figure 10: Frontier molecular orbital energy diagram of 1^H carbene and N_2

Thus, the donation of σ electron pair of carbene to this orbital would be difficult. Energies required for different electronic transitions are given in Figure 10. The minimum energy required for the brown path is 7.87 eV which is significantly higher than the green path. The minimum energy required for the green path is 6.48 eV. Thus, the σ donation and π acceptance behavior of carbene are not observed here (brown path). This reaction follows the green path. In the green path, the HOMO electron pair of carbene is excited to the LUMO which is followed by the HOMO electron donation of N_2. The complex is further stabilized by the back donation of electrons from carbene to the vacant π^* orbital of N_2. This is confirmed by the charge distribution of the diazo derivative where the central nitrogen is positively charged.

3.2.4 Detection of electron flow during activation reaction employing molecular Handycam technique

To validate the proposed electronic mechanism of the carbene$-N_2$ reaction depicted above, the change in the HOMO electron cloud of the diazo derivative formation along the reaction path is captured and construed in Figure 11. Single-point energy calculation is carried out for selected geometries obtained from the IRC study. Since electronic wave functions are optimized independently at a particular geometry, the pictures of electron distribution of HOMOs at different geometries collectively mimic the snapshots of the flow of electrons

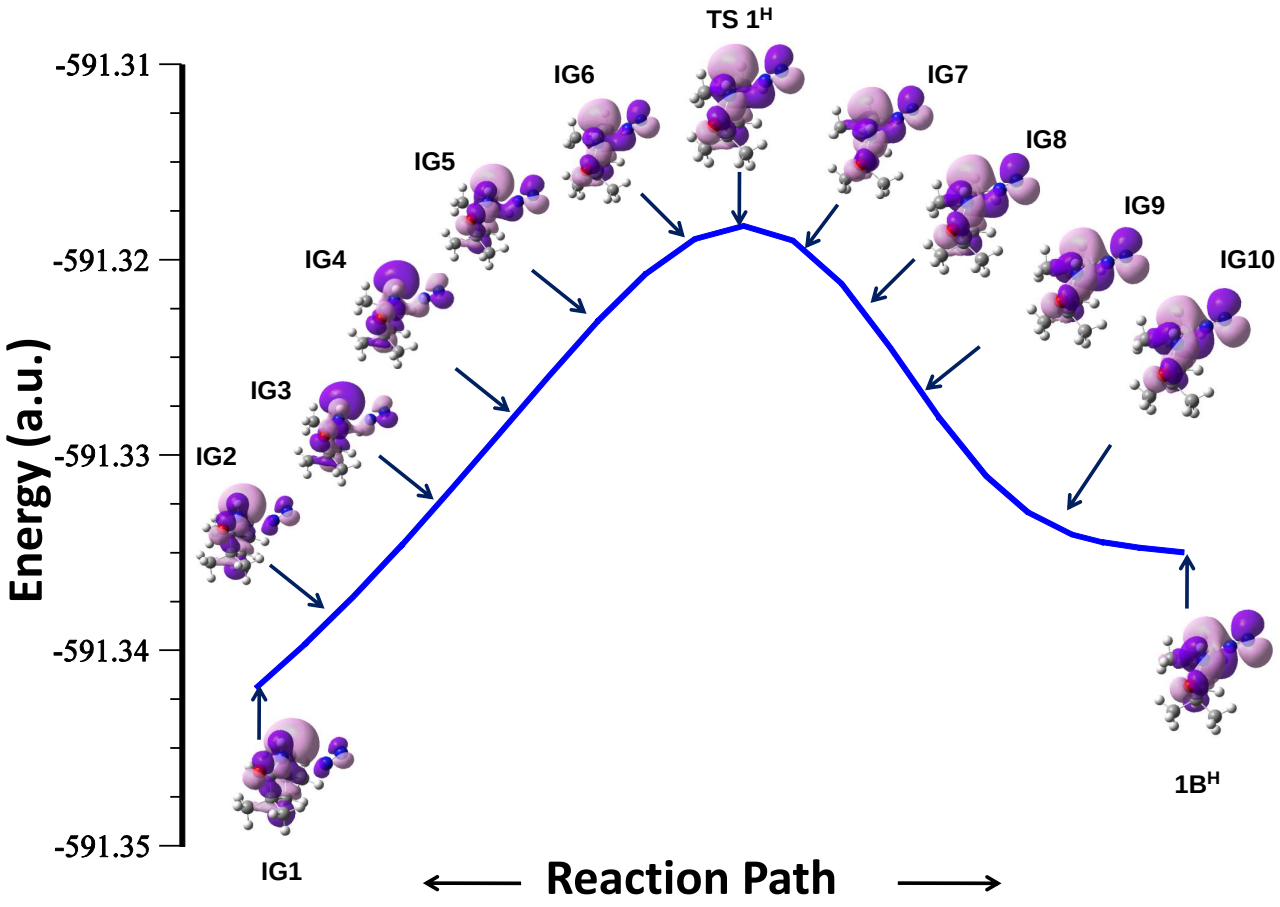

Figure 11: Change of HOMO electron cloud along IRC

during the reaction. Henceforth, this approach may be considered as the *Molecular Handycam*. These orbital pictures reflect the change of electron cloud along the reaction coordinate beyond the Born−Oppenheimer approximation.

It is observed from Figure 11 that at first the σ electron cloud of N_2 started to elongate towards carbene carbon (IG2) when two reactants get closer. The orbital overlap between carbene carbon and N_2 is observed at the initial stage of the reaction (IG3). Along the reactant path, the extent of the orbital overlap is enhanced with the advancement of the reaction till the transition state is attained. There is no significant change in this orbital overlap along the product path. The formation of the back bonding started after crossing the transition state. The back bonding is predominantly governed by the elongation of the HOMO electron cloud over the carbene carbon (IG8) towards the π orbital of nitrogen. The overlap is almost completed at IG10 which is very close to the product. From these observations, it may be concluded that this reaction occurs through the σ electron donation of nitrogen and back donation of carbene. However, there is a significant time gap between the completion of bonding and the beginning of the back−bonding. We may consider this state as the rest phase of the reaction where no orbital electron movement is observed. For this reaction, the rest phase is observed at the transition state itself.

3.2.5 Evanescent optical absorbance phenomenon

The optical absorbance property of carbene−N_2 adduct along the reaction path is studied. The intermediate geometries along the reaction coordinate are extracted from the IRC computation. Time-dependent density functional computations are carried out for selective geometries to obtain the optical absorbance behavior along the reaction path. Computed results are presented in Figure 12.

It is observed that the reactants and product have no significant absorbance in the visible region. However, due to the advancement of the reaction, a peak within the visible region appears at 474 nm with very low absorbance intensity. A blue shift of this peak is observed

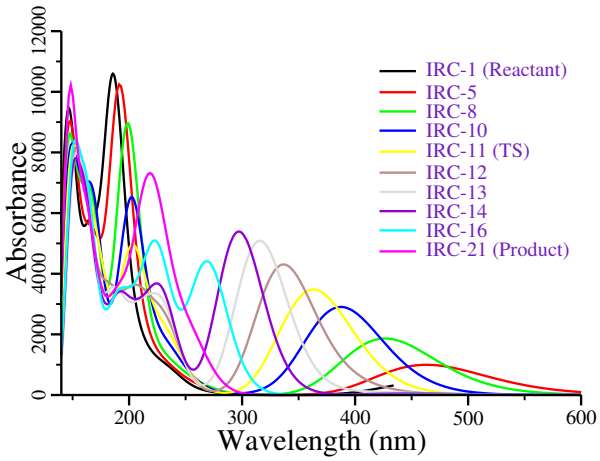

Figure 12: Change of optical absorbance behaviour along reaction path of nitrogen activation reaction

with the increase in absorbance towards the transition state. The absorbance reached the maximum just before reaching the transition state (IG6 of Figure 11). The peak position is 387 nm and the oscillator strength is 0.07. Crossing this step, absorption falls in the UV region. Before the completion of the reaction, another absorption maximum is observed at 297 nm with an oscillator strength of 0.133 which exists in the UV region.

This study posits that though the reactants and products of a reaction are inactive in a particular region of electromagnetic radiation, they may exhibit activity in that zone during a chemical reaction. This type of optical absorbance behavior may be termed the *Evanescent optical absorbance phenomenon* of a reaction. If the reaction is irradiated with electromagnetic radiation where the evanescent optical activity is observed, a new type of emission property may be accomplished.

3.2.6 Origin of evanescent optical absorbance phenomenon of carbene$-N_2$ reaction

To track down the origin of the evanescent optical absorbance phenomenon of carbene$-N_2$ reaction, the orbitals' involvement in the respective absorptions is hunted out. The change of oscillator strength of the respective transitions is plotted along the reaction coordinate which is shown in Figure 13. It is observed that the absorptions are due to two different

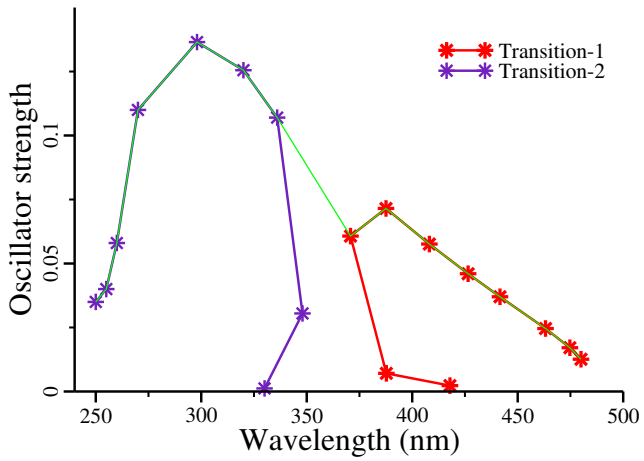

Figure 13: Origin of evanescent optical absorbance phenomenon of carbene−N_2 reaction

kinds of transitions. HOMO to LUMO transition is responsible for the initial absorbance which occurs along the reactant path and LUMO to HOMO transition is observed along the product path. These satisfy our previous observations that donation and back donation of electrons occur before and after the crossing of the transition state. It also attests to the carbene $-$ N_2 binding mechanism proposed in section 3.2.2. It is also concluded that bonding requires lower energy than back bonding which is obvious.

3.2.7 Modelling of new carbene

Among all carbenes studied so far, 1^{CN} carbene is found the most effective for N_2 activation which is due to the presence of the $C = O$ group. Thus, a carbene is modeled by adding one more $C = O$ group to 1^{CN} carbene which is presented in Figure 14. Nitrogen activation reaction is studied with this carbene. The effect of substitution is also studied. The energy profile diagram for the activation reaction with this carbene (5^R) is presented in Figure 15.

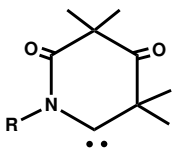

Figure 14: Modeled carbene 5^R ($R = CF_3$, CN, H, Me, OMe, Ph, tBu)

The reaction between N_2 and carbene 5^R (Figure 15) follows similar trends as it is

observed for four other carbenes. First, the pre-complex $5A^R$ is formed through an endergonic process. The very next step is the transformation of $5A^R$ to $5B^R$ through a transition state $TS5^R$. The effect of substitution is almost the same for this carbene too. The activation energy barrier for different substituents obeys the order $CN < CF_3 < H < Ph < Me < OMe < tBu$. The lowest and the highest activation energy barrier for this step is 20.8 Kcal/mol and 27.4 Kcal/mol for 5^{CN} and 5^{tBu} respectively. This is very interesting because the highest activation energy is only 27.4 kcal/mol which implies that these carbenes are able to activate N_2 at room temperature. This result is also inspiring because the change in the carbene frame through the addition of one $C = O$ group is found effective for lowering the activation energy. The high activity of carbene due to the presence of the $C = O$ group in the carbene frame and the CN functional group connected to the heteroatom of the carbene frame support our conclusion regarding the binding nature discussed earlier.

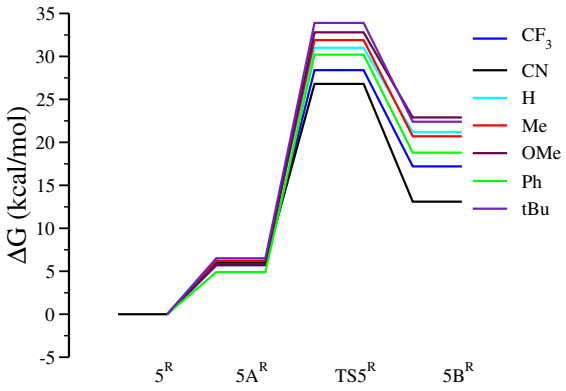

Figure 15: Energy profile diagram for the reaction of carbene 5^R ($R = CF_3$, CN, H, Me, OMe, Ph, tBu) with N_2.

Unfortunately, the free energy change of this process is still positive for all of the substituents. The stability order of the diazo derivative is $CN > CF_3 > Ph > Me > H > tBu > OMe$. The most stable diazo derivative is for the 5^{CN} (free energy change is 13.5 kcal/mol). At present, there is no clue to find a better carbene that would be effective for N_2 activation at room temperature and produce a thermodynamically stable diazo derivative. Thus, alternative techniques are explored to reach our goal.

3.3 Stabilization of activated N_2

Our propensity is to activate the N_2 by carbene at an ambient condition and stabilize the diazo derivatives. This is achieved in three different ways − reducing the diazo derivative by hydrogen, through the formation of azo derivative, and employing mutation of the heteroatom of N-heterocyclic carbene.

3.3.1 Reduction of diazo compound by H_2 molecule

To stabilize the diazo derivative of the model carbene, $5B^{CN}$, reduction of this derivative by hydrogen is studied. The result is presented in Figure 16. This study is performed because our prime goal is to convert molecular nitrogen and hydrogen to ammonia. Enthusiastically it is observed that the reaction-free energy for this step (-22.6 kcal/mol) and the total process as well is negative (-9.5 kcal/mol). Thus, thermodynamically this process is feasible. However, the activation energy for the reduction of the diazo derivative is quite high (59.5 kcal/mol) which indicates that this reaction may occur at a higher temperature.

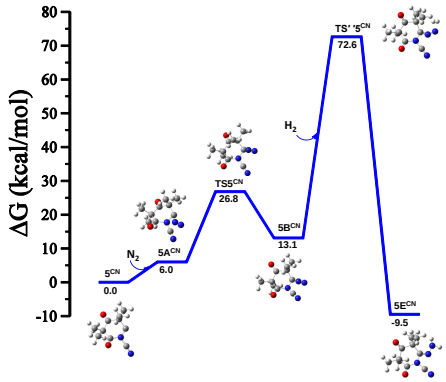

Figure 16: Reduction of diazo derivative, $5B^{CN}$ by H_2 molecule

3.3.2 Stabilization of activated N_2 through the formation of azo derivative

It is reported that the reaction of two molecules of carbene with SO_2 is fruitful to convert the captured SO_2 to valuable chemicals.[7] This approach is exercised for the present study. The schematic representation of this reaction is shown in Figure 17. The cyanide substituted

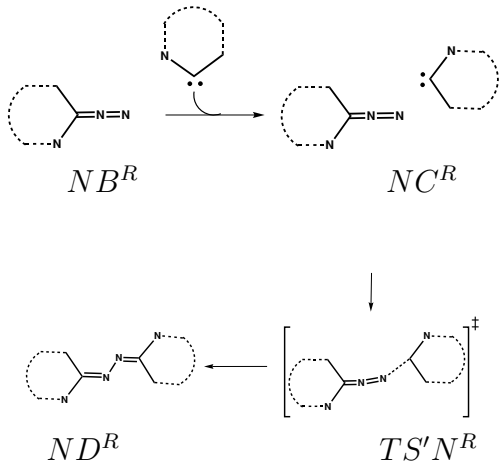

Figure 17: Schematic representation of the reaction of N-heterocyclic carbene with diazo derivative of the same carbene. ($N = 5$; R= CN)

model carbene (5^{CN}) is employed for this purpose. For this study, the second carbene is allowed to react with the diazo derivative ($5B^{CN}$). The complete (including the formation of the diazo derivative) energy profile diagram of this reaction is presented in Figure 18.

The reaction of the second carbene with the diazo derivative is exactly the same as it is observed for the reaction between the carbene and N_2. At first a pre-complex ($5C^{CN}$) is formed which is converted to the azo derivative ($5D^{CN}$) through a transition state $TS'5^{CN}$. The only difference which is observed in the reaction of the second carbene molecule with the diazo derivative is the lowering of the activation energy and the stabilization of the product.

The energy required for the formation of the pre-complex ($5C^{CN}$) is 4.9 kcal/mol and for the transition state is 5.7 kcal/mol. This implies that the reaction of the second carbene molecule is more facile than the first one. It is also observed that the azo derivative is highly stable. The Gibbs' free energy change of the total process is -54.8 kcal/mol. Thus, we may conclude that in the presence of a high concentration of carbene, the formation of the azo derivative will be predominant over the diazo derivative.

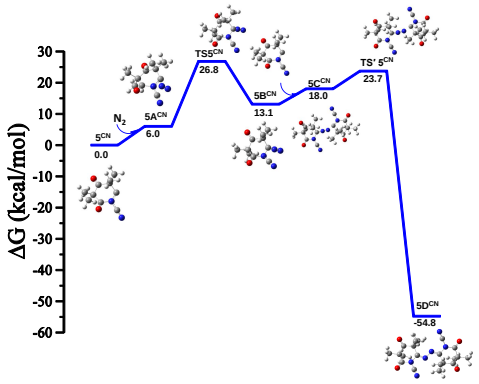

Figure 18: Energy profile diagram for the reaction of carbene 5^{CN} with N_2.

3.3.3 Stabilization of activated nitrogen through the Mutation of the hetero atom (N-heterocyclic carbene → P-heterocyclic carbene)

It is found that 5^{CN} carbene is highly effective to activate nitrogen. However, Gibbs' free energy change for the formation of the diazo derivative is positive. Though the reaction of the second carbene molecule is effective to convert the diazo derivative to a highly stable azo derivative (free energy change is -54.8 kcal/mol) further investigation is carried forward by mutating the heteroatom of carbene to obtain a thermodynamically stable diazo derivative. For this study, the hetero nitrogen of 5^{CN} carbene is substituted by phosphorus to have another model carbene (6^{CN}) presented in Figure 19. Phosphorus is chosen for this purpose as it is the same group element (below nitrogen) and it is also a trivalent atom.

A comparison between the energy profile diagrams of the reactions of 5^{CN} and 6^{CN} carbenes with nitrogen is presented in Figure 20. It is observed that the reaction of P-heterocyclic carbene (PHC) with nitrogen is very similar to N-heterocyclic carbene. The reaction occurs through the formation of the pre-complex, transition state and diazo derivative. There is no significant change in the energy required for the formation of the pre-complex ($6A^{CN}$). However, an enthusiastic change in activation energy is observed. The required activation energy for the formation of the transition state ($TS6^{CN}$) is only 11.6 kcal/mol which is lower by 9.2 kcal/mol compared to its nitrogen analog. Thus, PHC is highly reactive to nitrogen even under ambient conditions. Not only that, the diazo derivative of PHC ($6B^{CN}$)

is thermodynamically stable too. The Gibbs' free energy change for this process is −10.1 kcal/mol. From this study, it may be concluded that a proper mutation at the heteroatom may reduce the activation energy of the reaction and at the same time, it may increase the stability of the product.

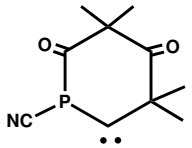

Figure 19: Modeled carbene 6^{CN}

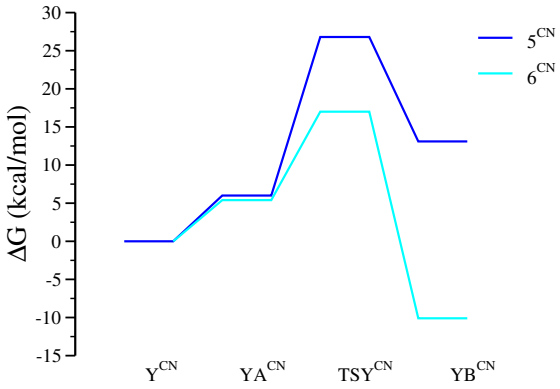

Figure 20: Energy profile diagram for the reaction of carbene Y^{CN} (Y=5, 6) with N_2.

3.4 Conversion of diazo compound to ammonia

So far, our study was limited to the activation of nitrogen and stabilization of the diazo derivative. It is observed that the model carbene (6^{CN}) is an efficient candidate for the sequestering of nitrogen at an ambient condition to yield a stable diazo derivative. Thus, the reduction of the diazo derivative is studied further. This reduction process is carried out with a fictitious reducing agent. For the computation process, only the H^+ ion and e are considered. The schematic reaction is presented in Equation 1.

$$6B^{CN} + 6H^+ + 6e^- \rightarrow 6^{CN} + 2NH_3 \tag{1}$$

The catalytic cycle and energy profile diagram for the formation of ammonia by employing 6^{CN} carbene as a catalyst, is depicted in Figure 21 and Figure 22 respectively.

$6B^{CN}$ is converted to 6^{CN} and two molecules of ammonia through a series of successive reductions to complete the catalytic circle. In this study, H (as hydrogen atom) is added in each step. It is observed that all H addition are barrier-less processes and exergonic. Here, all steps of the reduction process are barrier-less due to the fact that only the addition of a hydrogen atom is considered. However, depending upon the nature of the hydrogen carrier or the reducing agent, there may exist an activation energy barrier for one or more steps. Though, the reduction process will remain exergonic. Thus, by employing an efficient reducing agent, the conversation of $6B^{CN}$ to 6^{CN} and NH_3 would be highly possible.

The addition of hydrogen occurs first at the terminal nitrogen. Till one molecule of ammonia is released, the addition of hydrogen occurs to the terminal nitrogen. After the release of one molecule of ammonia, the addition of hydrogen atoms occurs to the second nitrogen atom one by one until the second molecule of ammonia is released. Here, the reaction may occur through the ionization of a hydrogen atom to yield H^+ and electron (e). In the diazo derivative, the central nitrogen atom is positively charged. Thus, it attracts the electron of the hydrogen atom to form H^+ which is attracted by the terminal nitrogen. Thus, the addition of a hydrogen atom takes place at the terminal nitrogen atom.

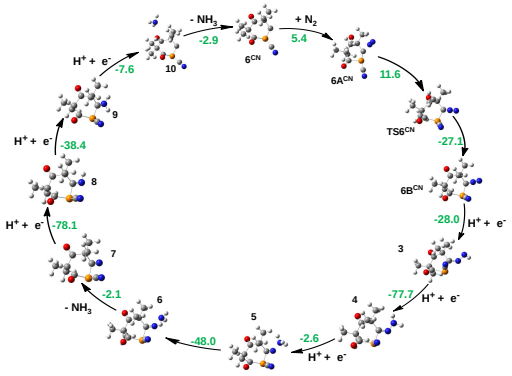

Figure 21: Catalytic Cycle.

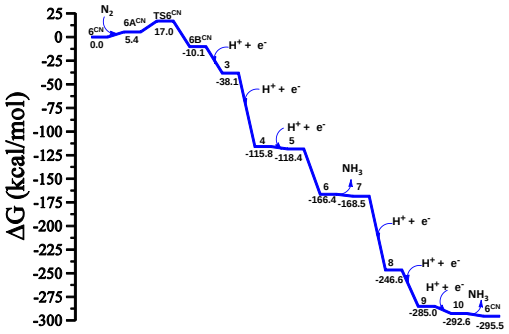

Figure 22: Energy profile.

3.5 Summary of the results

In the present inquisition, the reaction of N_2 with four principal carbenes(1^R, 2^R, 3^R, 4^R) with seven substituents ($R = CF_3$, CN, H, Me, OMe, Ph, tBu) are studied (Sec. 3.1). It is observed that among 28 carbenes 1^{CN} is the better candidate for N_2 sequestering. But the Gibbs' free energy of reaction of the diazo derivative of all carbenes including 1^{CN} is positive. Therefore, the further quest was continued. A set of new carbenes (5^R, $R = CF_3$, CN, H, Me, OMe, Ph, tBu) analogous to carbene 1^R, are also exploited for the fixation of nitrogen (Sec. 3.2). It is noticed that 5^{CN} is an affluent candidate for N_2 activation. However, the Gibbs' free energy change for the formation of $5B^{CN}$ remains positive. Thus, further explorations were demanded which were fulfilled by the reduction of diazo derivative by hydrogen, formation of azo derivative and mutation at the heteroatom of the carbene (Sec. 3.3). The stabilization of the diazo derivative is attempted by the addition of molecular hydrogen. Though the initial aim was fulfilled, the activation energy of this process is very high. For the formation of the azo derivative, carbene (5^{CN}) was added to the diazo derivative ($5B^{CN}$). Through this process a stable azo derivative ($5D^{CN}$) was formed having -54.8 kcal/mol reaction free energy.

For the mutation of heteroatom of N-heterocyclic carbene, the nitrogen atom is replaced by the phosphorous atom of 5^{CN} carbene. This carbene is termed as 6^{CN} carbene. The reaction of N_2 with 6^{CN} was also studied. It is observed that activation energy and reaction-

free energy of this reaction are 11.6 kcal/mol and -10.1 kcal/mol respectively. Among all carbenes, the lowest activation energy for the formation of the diazo derivative is observed for the 6^{CN} carbene. This diazo derivative is the most stable too. Therefore, 6^{CN} is the best candidate for N_2 activation in our present Inquisition.

An explicit discussion about the bonding nature and the binding process of the carbene $-$ N_2 reaction is represented in Sec 3.2. It is observed that the diazo derivative is formed through the bonding $-$ back-bonding phenomena of carbene. The HOMO of carbene has the σ type symmetry and the LUMO of carbene has the π type symmetry, and at the same time, the HOMO of N_2 is a σ type orbital and the LUMO of N_2 is a π type orbital. Thus, the electron donation of carbene to nitrogen is not possible in a straightforward way. The electron transfer and bond formation may occur through a complex pathway. The analysis of the molecular orbitals unveils that at first, the HOMO electron pair of carbene excited to the LUMO of carbene then the HOMO electron pair of N_2 is donated to the vacant HOMO of the carbene. In this process, the bonding is taken place. It is observed that the bonding process is completed before the transition state is reached. After crossing the transition state, the back-bonding takes place. The excited electron pair of carbene is donated to the vacant π^* of N_2 to accomplish the back-bonding.

The possible conversion of the diazo derivative to ammonia is also studied and presented in Sec. 3.4. It is observed that 6^{CN} may act as a catalyst for the metamorphosis of N_2 to ammonia.

4 Conclusions

From the present study, it is concluded that by employing an appropriate carbene (6^{CN} in this study) molecular nitrogen may be sequestered and converted to ammonia by the successive reduction process. Carbene acts as a σ-acceptor and π-donor in this process. The electronic level investigation proclaimed that the bonding and the back bonding processes

are not instantaneous. These two processes occur at different stages of the reaction. The bonding takes place before reaching the transition state while the back bonding occurs after the transition state which implies that these two processes are independent of each other. There are a few more important outcomes from this quest. IRC trapping followed by TD-DFT computation may act as a molecular Handycam to understand a chemical reaction with greater precision. It is also demonstrated here that a chemical reaction may have a characteristic behavior of optical activity. These results may stimulate future experimental inquisitions.

Supporting Information Available

The optimized geometries of all compounds are available in the electronic supporting information file. A1. Electronic absorption at different geometries along the carbene-N2 reaction path A2. Z coordinates of the different complexes.

Conflicts of interest

The authors declare no competing financial interest.

Acknowledgements

R.L. acknowledges CSIR (CSIR file No. 09/921(0144)/2016-EMR-I), India for the financial support. A.K.T. acknowledges IISER Kolkata, project No. IISER-K/DoRD/R&P/2017-18/295 for the financial support.

References

(1) Parr, R. G.; Yang, W. "Density-functional theory of the electronic structure of molecules", *Annual review of physical chemistry* **1995,** *46,* 701–728.

(2) Bag, A. "Transition probability approach for direct calculation of coefficients of configuration interaction wave function", *Current Science* **2017,** 2325–2328.

(3) Bag, A.; Manohar, P. U.; Vaval, N.; Pal, S. "First-and second-order electrical properties computed at the FSMRCCSD level for excited states of closed-shell molecules using the constrained-variational approach", *The Journal of chemical physics* **2009,** *131,* 024102.

(4) Bag, A. *Linear response approach in FSMRCC for molecular property;* LAP Lambert Academic Publishing: 2016.

(5) Zhao, B.; Han, S.; Malbon, C. L.; Manthe, U.; Yarkony, D.; Guo, H.; others, "Full-dimensional quantum stereodynamics of the non-adiabatic quenching of OH (A2Σ+) by H2", *Nature chemistry* **2021,** *13,* 909–915.

(6) Balakrishnan, N.; Kalyanaraman, C.; Sathyamurthy, N. "Time-dependent quantum mechanical approach to reactive scattering and related processes", *Physics reports* **1997,** *280,* 79–144.

(7) Logdi, R.; Bag, A.; Tiwari, A. K. "Schematic Design of Metal-Free NHC-Mediated Sequestering and Complete Conversion of SO2 to Thiocarbonyl S-Oxide Derivatives at Room Temperature", *J. Phys. Chem. A* **2022,** .

(8) Qiu, W. *et al.* "High-performance artificial nitrogen fixation at ambient conditions using a metal-free electrocatalyst", *Nat. commun.* **2018,** *9,* 1–8.

(9) Smil, V. "Global population and the nitrogen cycle", *Scientific American* **1997,** *277,* 76–81.

(10) Jennings, J. R. *Catalytic ammonia synthesis: fundamentals and practice;* Springer Science & Business Media: 1991.

(11) Xin, X.; Douair, I.; Zhao, Y.; Wang, S.; Maron, L.; Zhu, C. "Dinitrogen cleavage by a heterometallic cluster featuring multiple uranium–rhodium bonds", *J. Am. Chem. Soc.* **2020,** *142,* 15004–15011.

(12) Gao, Y.; Li, G.; Deng, L. "Bis (dinitrogen) cobalt (- 1) complexes with NHC ligation: Synthesis, characterization, and their dinitrogen functionalization reactions affording side-on bound diazene complexes", *J. Am. Chem. Soc.* **2018,** *140,* 2239–2250.

(13) Rodriguez, M. M.; Bill, E.; Brennessel, W. W.; Holland, P. L. "N2 reduction and hydrogenation to ammonia by a molecular iron-potassium complex", *Science* **2011,** *334,* 780–783.

(14) Wang, P.; Douair, I.; Zhao, Y.; Wang, S.; Zhu, J.; Maron, L.; Zhu, C. "Facile Dinitrogen and Dioxygen Cleavage by a Uranium (III) Complex: Cooperativity Between the Non-Innocent Ligand and the Uranium Center", *Angew. Chem.* **2021,** *133,* 477–483.

(15) Lv, Z.-J.; Huang, Z.; Zhang, W.-X.; Xi, Z. "Scandium-promoted direct conversion of dinitrogen into hydrazine derivatives via n–c bond formation", *J. Am. Chem. Soc.* **2019,** *141,* 8773–8777.

(16) Lv, Z.-J.; Wei, J.; Zhang, W.-X.; Chen, P.; Deng, D.; Shi, Z.-J.; Xi, Z. "Direct transformation of dinitrogen: synthesis of N-containing organic compounds via N- C bond formation", *Natl. Sci. Rev.* **2020,** *7,* 1564–1583.

(17) Shima, T.; Hu, S.; Luo, G.; Kang, X.; Luo, Y.; Hou, Z. "Dinitrogen cleavage and hydrogenation by a trinuclear titanium polyhydride complex", *Science* **2013,** *340,* 1549–1552.

(18) Pool, J. A.; Lobkovsky, E.; Chirik, P. J. "Hydrogenation and cleavage of dinitrogen to ammonia with a zirconium complex", *Nature* **2004,** *427,* 527–530.

(19) McWilliams, S. F.; Holland, P. L. "Dinitrogen binding and cleavage by multinuclear iron complexes", *Acc.Chem. Res.* **2015,** *48,* 2059–2065.

(20) Falcone, M.; Chatelain, L.; Scopelliti, R.; Živković, I.; Mazzanti, M. "Nitrogen reduction and functionalization by a multimetallic uranium nitride complex", *Nature* **2017,** *547,* 332–335.

(21) Ashida, Y.; Arashiba, K.; Nakajima, K.; Nishibayashi, Y. "Molybdenum-catalysed ammonia production with samarium diiodide and alcohols or water", *Nature* **2019,** *568,* 536–540.

(22) Khan, S. N.; Kalemos, A.; Miliordos, E. "Metal-Free Activation of N2 by Persistent Carbene Pairs: An Ab Initio Investigation", *J. Phys. Chem. C* **2019,** *123,* 21548–21553.

(23) Wang, C.-H.; Yin, Z.-B.; Wei, J.; Zhang, W.-X.; Xi, Z. "Outlook of nitrogen fixation by carbene", *Tetrahedron* **2020,** *76,* 131703.

(24) Rouf, A. M.; Huang, Y.; Dong, S.; Zhu, J. "Systematic Design of a Frustrated Lewis Pair Containing Methyleneborane and Carbene for Dinitrogen Activation", *Inorg. Chem.* **2021,** *60,* 5598–5606.

(25) Park, S.-W.; Chun, Y.; Cho, S. J.; Lee, S.; Kim, K. S. "Design of carbene-based organocatalysts for nitrogen fixation: theoretical study", *J. Chem. Theory Comput.* **2012,** *8,* 1983–1988.

(26) Légaré, M.-A.; Bélanger-Chabot, G.; Dewhurst, R. D.; Welz, E.; Krummenacher, I.; Engels, B.; Braunschweig, H. "Nitrogen fixation and reduction at boron", *Science* **2018,** *359,* 896–900.

(27) Légaré, M.-A.; Rang, M.; Bélanger-Chabot, G.; Schweizer, J. I.; Krummenacher, I.; Bertermann, R.; Arrowsmith, M.; Holthausen, M. C.; Braunschweig, H. "The reductive coupling of dinitrogen", *Science* **2019,** *363,* 1329–1332.

(28) Pichon, D. *et al.* "The debut of chiral cyclic (alkyl)(amino) carbenes (CAACs) in enantioselective catalysis", *Chem. Sci.* **2019,** *10,* 7807–7811.

(29) Ghafarian Shirazi, R.; Neese, F.; Pantazis, D. A.; Bistoni, G. "Physical nature of differential spin-state stabilization of carbenes by hydrogen and halogen bonding: A domain-based pair natural orbital coupled cluster study", *J. Phys. Chem. A* **2019,** *123,* 5081–5090.

(30) Gautam, N.; Logdi, R.; Sreejyothi, P.; Rajendran, N.; Tiwari, A. K.; Mandal, S. K. "Bicyclic (alkyl)(amino) carbene (BICAAC) as a metal-free catalyst for reduction of nitriles to amines", *Chem. Commun.* **2022,** *58,* 3047–3050.

(31) Day, B. M.; Pugh, T.; Hendriks, D.; Guerra, C. F.; Evans, D. J.; Bickelhaupt, F. M.; Layfield, R. A. "Normal-to-abnormal rearrangement and NHC activation in three-coordinate iron (II) carbene complexes", *J. Am. Chem. Soc.* **2013,** *135,* 13338–13341.

(32) Soleilhavoup, M.; Bertrand, G. "Cyclic (alkyl)(amino) carbenes (CAACs): stable carbenes on the rise", *Acc. Chem. Res.* **2015,** *48,* 256–266.

(33) Melaimi, M.; Jazzar, R.; Soleilhavoup, M.; Bertrand, G. "Cyclic (alkyl)(amino) carbenes (CAACs): recent developments", *Angew. Chem., Int. Ed.* **2017,** *56,* 10046–10068.

(34) Tomás-Mendivil, E.; Hansmann, M. M.; Weinstein, C. M.; Jazzar, R.; Melaimi, M.; Bertrand, G. "Bicyclic (alkyl)(amino) carbenes (BICAACs): Stable carbenes more ambiphilic than CAACs", *J. Am. Chem. Soc.* **2017,** *139,* 7753–7756.

(35) Nesterov, V.; Reiter, D.; Bag, P.; Frisch, P.; Holzner, R.; Porzelt, A.; Inoue, S. "NHCs in main group chemistry", *Chem. Rev.* **2018,** *118,* 9678–9842.

(36) Danopoulos, A. A.; Simler, T.; Braunstein, P. "N-heterocyclic carbene complexes of copper, nickel, and cobalt", *Chem. Rev.* **2019,** *119,* 3730–3961.

(37) Logdi, R.; Bag, A.; Tiwari, A. K. "DFT based engineering of N-heterocyclic carbenes to exacerbate its activity for SO2 fixation and storage", *J. Mol. Graphics Modell.* **2019,** *93,* 107437.

(38) Logdi, R.; Bag, A.; Tiwari, A. K. "Competitive Reactivity of SO2 and NO2 with N-Heterocyclic Carbene: A Mechanistic Study", *J. Phys. Chem. A* **2021,** *125,* 5718–5725.

(39) Moore, C. B.; Pimentel, G. C. "Matrix reaction of methylene with nitrogen to form diazomethane", *J. Chem. Phys.* **1964,** *41,* 3504–3509.

(40) Shilov, A.; Shteinman, A.; Tjabin, M. "Reaction of carbenes with molecular nitrogen", *Tetrahedron Lett.* **1968,** *9,* 4177–4180.

(41) Grieve, D. M.; Lewis, G. E.; Ravenscroft, M. D.; Skrabal, P.; Sonoda, T.; Szele, I.; Zollinger, H. "Reactivity of carbenes and related compounds towards molecular nitrogen", *Hel. Chim. Acta.* **1985,** *68,* 1427–1443.

(42) Liu, M. T.; Choe, Y.-K.; Kimura, M.; Kobayashi, K.; Nagase, S.; Wakahara, T.; Niino, Y.; Ishitsuka, M. O.; Maeda, Y.; Akasaka, T. "Effect of substituents on the thermal decomposition of diazirines: Experimental and computational studies", *J. Org. Chem.* **2003,** *68,* 7471–7478.

(43) Zhu, J. "Rational Design of a Carbon-Boron Frustrated Lewis Pair for Metal-free Dinitrogen Activation", *Chem. Asian. J.* **2019,** *14,* 1413–1417.

(44) Rouf, A. M.; Dai, C.; Xu, F.; Zhu, J. "Dinitrogen activation by tricoordinated boron species: A systematic design", *Adv. Theory Simul.* **2020,** *3,* 1900205.

(45) Rouf, A. M.; Dai, C.; Dong, S.; Zhu, J. "Screening Borane Species for Dinitrogen Activation", *Inorg. Chem.* **2020,** *59,* 11770–11781.

(46) Yang, L.; Wang, H. "Recent Advances in Carbon Dioxide Capture, Fixation, and Activation by using N-Heterocyclic Carbenes", *ChemSusChem* **2014,** *7,* 962–998.

(47) Huang, F.; Lu, G.; Zhao, L.; Li, H.; Wang, Z.-X. "The catalytic role of N-heterocyclic carbene in a metal-free conversion of carbon dioxide into methanol: a computational mechanism study", *J. Am. Chem. Soc.* **2010,** *132,* 12388–12396.

(48) Hota, P. K.; Sau, S. C.; Mandal, S. K. "Metal-Free Catalytic Formylation of Amides Using CO2 under Ambient Conditions", *ACS Catal.* **2018,** *8,* 11999–12003.

(49) Denning, D. M.; Falvey, D. E. "Substituent and Solvent Effects on the Stability of N-Heterocyclic Carbene Complexes with CO2", *J. Org. Chem.* **2017,** *82,* 1552–1557.

(50) Zhao, Y.; Truhlar, D. G. "The M06 suite of density functionals for main group thermochemistry, thermochemical kinetics, noncovalent interactions, excited states, and transition elements: two new functionals and systematic testing of four M06-class functionals and 12 other functionals", *Theo. Chem. Acc.* **2008,** *120,* 215–241.

(51) Frisch, M. J. *et al.* "Gaussian 09 Revision D.01", Gaussian Inc. Wallingford CT 2009.

(52) Laurent, A. D.; Jacquemin, D. "TD-DFT benchmarks: a review", *International Journal of Quantum Chemistry* **2013,** *113,* 2019–2039.

Graphical TOC Entry